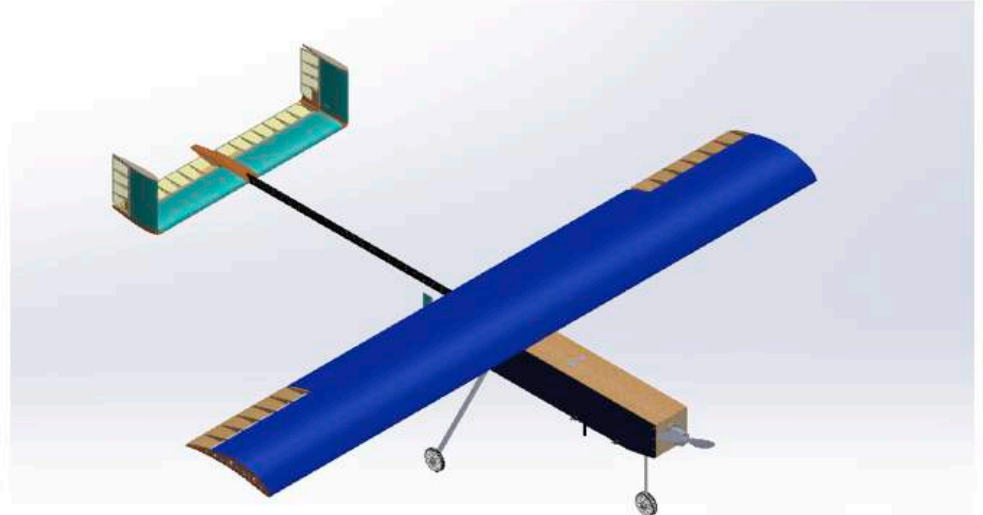




Advanced Modeling Aeronautics Team

Advanced Class, Team 218



University of California, Davis

AMAT 2019

Captain/ Fuselage Lead
Captain/ Empennage Lead
Captain/ Wing Lead
CDA Lead
Landing Gear Lead
Mission Specialist Lead
Mission Specialist Lead
Drop Mechanism Lead

Safa Bakhshi
Anthony Goldstone
Linda Wu
Luis Zarate-Sanchez
Edgardo Rivera Godoy
Savannah Buchner
Kylie Cooper
Brett Hecker

Team Members

William Britten
Louk Goldberg
Zoren Habana
Attila Hegedus
Jiawei Jiang

Heather Lynch
Elitt Noguera
Vinh Nguyen
Matthew Pena
Ryan Silva

Thalia Telles
Nathan Tran
Jordon Won

Faculty Advisers

Stephen K. Robinson, PhD Valeria La Saponara, PhD

APPENDIX A

STATEMENT OF COMPLIANCE

Certification of Qualification

Team Name Advanced Modeling Aeronautics Team Team Number 218


School UC Davis


Faculty Advisor Valeria La Saponara

Faculty Advisor's
Email vlasaponara@ucdavis.edu


Statement of Compliance



As faculty Adviser:

 (Initial) I certify that the registered team members are enrolled in collegiate courses.

 (Initial) I certify that this team has designed and constructed the radio controlled aircraft in the past nine (9) months with the intention to use this radio controlled aircraft in the **2019** SAE Aero Design competition, without direct assistance from professional engineers, R/C model experts, and/or related professionals.

 (Initial) I certify that this year's Design Report has original content written by members of this year's team.

 (Initial) I certify that all reused content have been properly referenced and is in compliance with the University's plagiarism and reuse policies.

 
Signature of Faculty Advisor

Ph: 530-754-8938


Signature of Team Captain

Note: A copy of this statement needs to be included in your Design Report as page 2 (Reference Section 4.3)

Contents

1	Executive Summary	5
2	Schedule Summary	5
3	Mission Analysis	6
3.1	Environmental Considerations	6
3.2	Competitive Scoring and Strategy Analysis	6
4	Design Features and Detail	8
4.1	Design Overview	8
4.2	Wings	8
4.3	Colonist Delivery Aircraft	11
4.3.1	Design Process	11
4.3.2	Wings	11
4.3.3	Empennage	12
4.3.4	Fuselage	13
4.4	Electronics	14
4.4.1	Power Circuit	14
4.4.2	Data Acquisition System	14
4.4.3	CDA Circuit	15
4.5	Drop Mechanism	15
4.5.1	Dynamic Payloads	15
4.6	Empennage	17
4.7	Fuselage	19
4.7.1	Static Payload	20
4.8	Landing Gear	20
5	Analysis	21
5.1	Analytical Tools Used	21
5.2	Dynamic and Static Stability	22
5.2.1	Longitudinal Stability	22
5.2.2	Lateral Stability and Directional Stability	23
5.3	Control Surface Sizing	23
5.4	Servo Sizing	23
5.5	Drag, Thrust, Takeoff, and Lifting Performance	24
5.6	Mass Breakdown	25
5.7	CDA Analysis	25
5.7.1	Lift Performance	25
5.7.2	Stability	26
6	Manufacturing	27
6.1	Composite Manufacturing	27
6.2	Additive Manufacturing	27
7	Conclusion	28
8	References	28

List of Figures

1	Proposed Schedule	6
2	Scoring Optimization Plot with Drop Accuracy of 20%	6
3	Flight Path	7
4	Eppler 423	8
5	Lift and Drag Polars for Eppler 423	9
6	Composite Laminate	10
7	Wing Assembly	10
8	Spar Bending Safety Factor	10
9	Clark Y Airfoil	12
10	NACA 0008 Airfoil	12
11	CDA Fuselage	13
12	Power Circuit	14
13	Data Acquisition System	15
14	CDA Circuit	15
15	Habitat Drop Mechanism Open	16
16	Habitat Drop Mechanism Closed	16
17	CDA Drop Mechanism	17
18	SolidWorks CAD Render of Exposed U-tail Empennage	18
19	SolidWorks CAD render of the fuselage with bulkheads and side panels showing	19
20	Nylon/Carbon Fiber Composite Landing Gear Wheel	21
21	Short Period, Phugoid, and Roll Stability Plots	22
22	Aileron Sizing for Gust Loading Conditions	23
23	Dyanamic Thrust Curve	24
24	Take off distance and velocity	24
25	Aerodynamic Visual of CDA	25
26	CDA Glide Polar	25
27	Side View of CDA	26
28	Carbon Fiber Layup on the Spars	27

List of Tables

1	Key Aircraft Parameters	8
2	Trade Study for Wing Composition	9
3	Design Matrix for Wing Configuration	11
4	Design Matrix for Empennage Configuration	11
5	Trade Study for Empennage Configuration	18
6	Trade Study for Empennage Composition	19
7	Trade Study for Fuselage Configuration	20
8	Trade Study for Landing Gear Material	21
9	Static Margin for Various Configurations	22
10	Servo Sizing	24
11	Zero Lift Drag Breakdown	24
12	Lift, Drag, and Thrust during Cruise and Takeoff	25
13	Mass Breakdown	25
14	Icarus' Dynamic Stability	26

Nomenclature

	$C_{L\alpha}$	Lift Curve Slope
α		Angle of Attack
	$C_{L\delta\alpha}$	Aileron Control Power
AC		Plane Aerodynamic Center
	$C_{M\alpha}$	Stability Derivative
AR		Aspect Ratio
	CG	Center of Gravity
C_D		Coefficient of Drag
	$MTOW$	Maximum Takeoff Weight
C_L		Coefficient of Lift
	NP	Neutral Point
C_M		Pitching Moment Coefficient
	SM	Static Margin
C_{D_0}		Zero Lift Coefficient of Drag
	TO	Take Off

1 Executive Summary

The Advanced Modeling Aeronautics Team's entry into the 2019 SAE Aero Design Competition includes Daedalus, our primary aircraft, and Icarus, our colonist delivery aircraft (CDA). This year's competition diverges from the simple drop missions of years past; instead it features a challenging colonist delivery mission, necessitating tight requirements management as well as sophisticated drop mechanism and electronic systems. Other changes to the competition includes switching from a gas-powered engine to an electric motor and inclusion of a 750W power limiter.

The team approached the design with the mission and competition requirements in mind, while balancing trades of manufacturability and cost. After many design iterations, Daedalus sports a high wing with an 8ft wingspan, a length of 7.25 ft tip-to-tail, and an U-tail. Three separate drop mechanisms were designed and integrated with the fuselage and wings. The water supply drop mechanism is a sling retained by a removable pin. The CDA mechanism is an open slot at the rear of the main craft which the CDA fits into. Each wing carries a habitat in an actuated acrylic claw, which opens to release the payload. The empty aircraft weighs 12.8lbs and when fully laden, carries 2 lbs of static payload, 2 habitats (Nerf Sports Vortex Aero Howler), a 1L bottle of water, and 1 CDA. The team opted to place the habitats on the wings, thereby reducing necessary fuselage volume.

The design of the aircraft was conducted using SolidWorks for CAD and MATLAB, XFLR, XFOIL, and OpenVSP for analysis. Manufacturing processes include traditional machining methods (mill, lathe, and drill press), as well as 3D printing, laser cutting, CNC, and water jetting. This is the first year the landing gear is utilizing new 3D printing methods that create composite parts of nylon and continuous carbon fiber thread. Carbon fiber composite layup is used for its excellent strength to weight ratio in both the wing spars and fuselage structure.

2 Schedule Summary

Proper scheduling is a necessity to achieve project milestones for full-time college students. The team maintained scheduling using online calendars and Slack, as well as weekly meeting early in the project phase, tapering down to biweekly meetings as we left the design phase. Below is our initial proposed schedule from the onset of the project. Adjustments were made as appropriate along the way. Some issues we came across included pending budget approvals, forcing us to design with unknown budget constraints. The design portion took longer than

initially budgeted, and significant revisions occurred along the way.

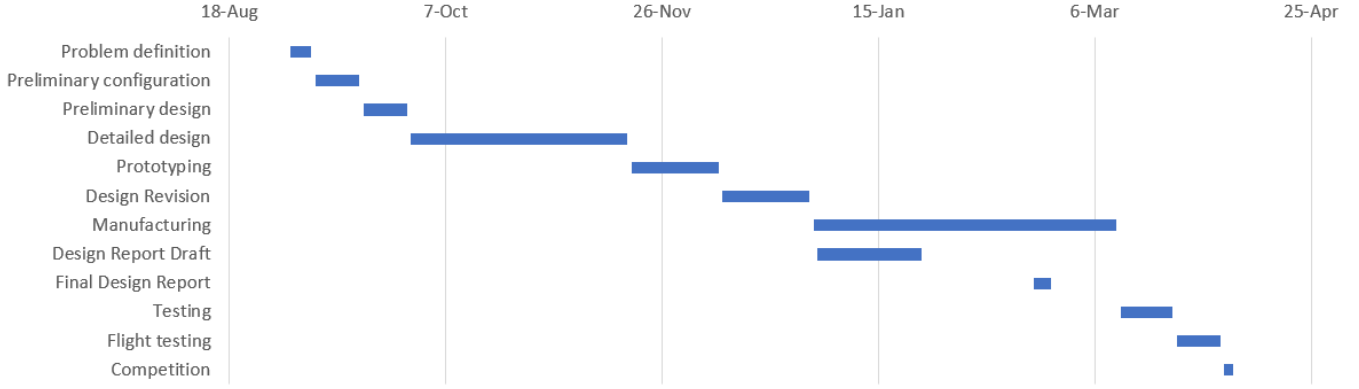


Figure 1: Proposed Schedule

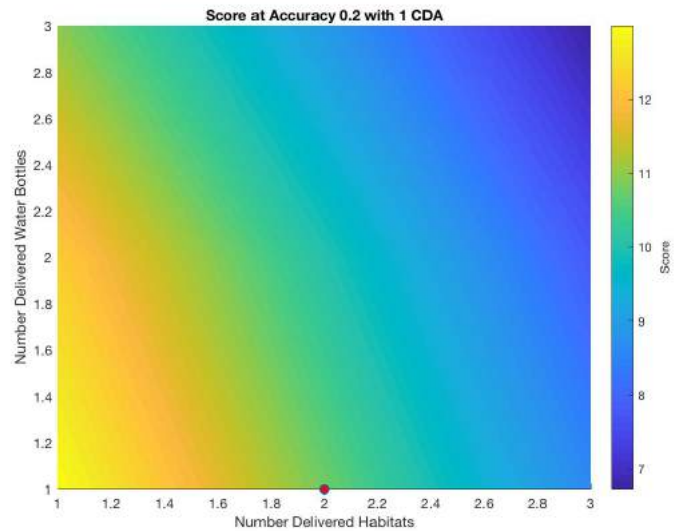
3 Mission Analysis

3.1 Environmental Considerations

The competition is located at Apollo 11 Field in Van Nuys, California which has a ground elevation of 705 ft. The plane must be able to fly to an altitude of over 805 ft for releasing payloads. Historical data shows that in April, Van Nuys has an average air density of 2.25×10^{-3} slug/ft³, an average wind speed of 11.14 ft/s, and an average maximum wind speed of 20.24 ft/s. Gust loading is a major consideration for the small aircraft as airframe load factor fluctuates with free stream velocity. Variable wind gusts must be survivable at any stage of flight.

3.2 Competitive Scoring and Strategy Analysis

The flight score is a combination of the colonist habitability and static payload carried, as shown in the equations below. In order to optimize the score, a study was done, with the results seen in Figure 2. The preliminary design considerations left the plane with around 6 lbs to be used for both static and dynamic payloads. Additionally, 1 CDA was selected as it would make the plane simpler and reduce hardware concerns.



An accuracy of 20% was generously estimated Figure 2: Scoring Optimization Plot with Drop Accuracy of 20%

based on previous years dropping accuracy. It

was determined that the optimal design would involve carrying the minimal amount of water and habitats as this allows more room for static payload to have guaranteed points. However, as the design progressed it was necessary for the habitats to be placed in the wings to reduce the fuselage size. In order to achieve a more stable flight, 2 habitats was selected for the final configuration so that one could be placed on each wing.

Scoring Equation:

$$FFS = \text{Final Flight Score} = \frac{N_c D}{15N} + \frac{2S_p}{N}$$

Where:

$$D = \text{Days of Habitability} = 25 \left(2^{1 - \text{Maximum}(\frac{N_C}{8N_H}, \frac{N_C}{N_W})} \right)$$

N = Total Number Rounds During the Competition

N_C = Total Number Colonists Delivered During the Competition

N_H = Total Number of Habitats Delivered During the Competition

N_w = Total Amount of Water (in fl oz) Delivered During the Competition

S_p = Total Static Payload (lbs) Delivered During the Competition

The mission involves dropping the CDA, a single one liter water bottle and two Nerf footballs into a target area. A maximum of two passes over the target are allowed. The plane takes off and lands upwind. In order to minimize the amount of turns the plane has to do, both dropping passes are also done in the upwind direction. None of the dropping mechanisms interfere with the others, so they could be completed in any order. The CDA has to be dropped from the furthest distance (greater than 200 feet). The Nerf footballs are more aerodynamic than the water bottles; thus, they fly further when dropped due to less drag.

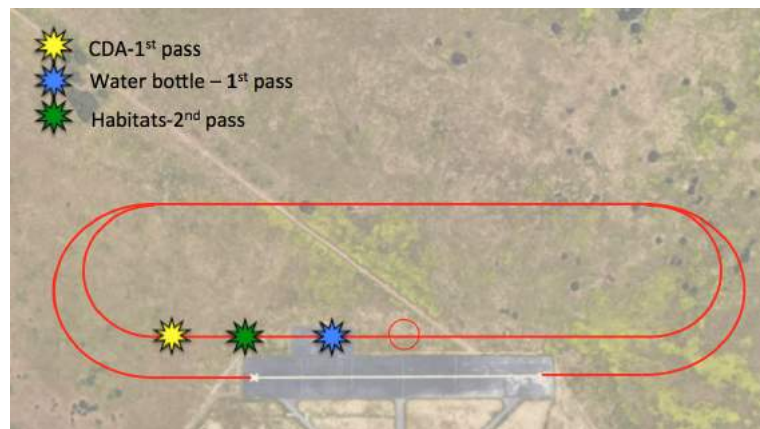


Figure 3: Flight Path

The goal in the dropping order is to ensure the highest precision possible. As drops will be initiated by the mission specialist, the time between each consecutive drop must be maximized

to minimize human reaction time error. Both flybys will be utilized. The first flyby will involve dropping the CDA and the water supply, while the second flyby will drop both habitats at once as seen in Figure 3.

4 Design Features and Detail

4.1 Design Overview

Below are the key parameters for the aircraft.

Table 1: Key Aircraft Parameters

Parameter	Value	Parameter	Value
Wingspan	$8ft$	MTOW	$25lbf$
Aspect Ratio	6.4	Empty Weight	$12.8lbf$
Horizontal Stabilizer Area	$240in^2$	Static Payload	$2lbf$
Vertical Tail Area	$120in^2$	Cruise Speed	$50ft/s$
Tail Aspect Ratio	4.18	Releasable Payload	1 CDA, 2 habitats, 1L water

4.2 Wings

Wing sizing was conducted with manufacturing and transportation limitations in mind. Different airfoils were considered, including the Selig 1223 and variants which have been used by the team in past years. The thin trailing edge of such high-lift airfoils complicates manufacturing and causes the wing trailing edge to be susceptible to damage. The Eppler 423 was chosen for its high-lift properties and thicker trailing edge which lends to easier manufacturing. Analysis on the airfoil was done using XFOIL and XFLR with Reynolds numbers in the range of $2 - 3E5$. $C_{L_{max}}$ was found to be 2.0032. Shown below in Figure 4 are the lift and drag polars for a 2D and 3D wing, as well as the Eppler 423 airfoil.

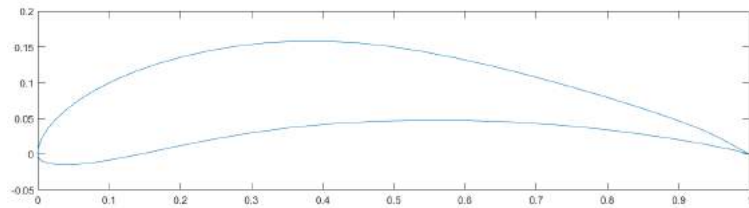


Figure 4: Eppler 423

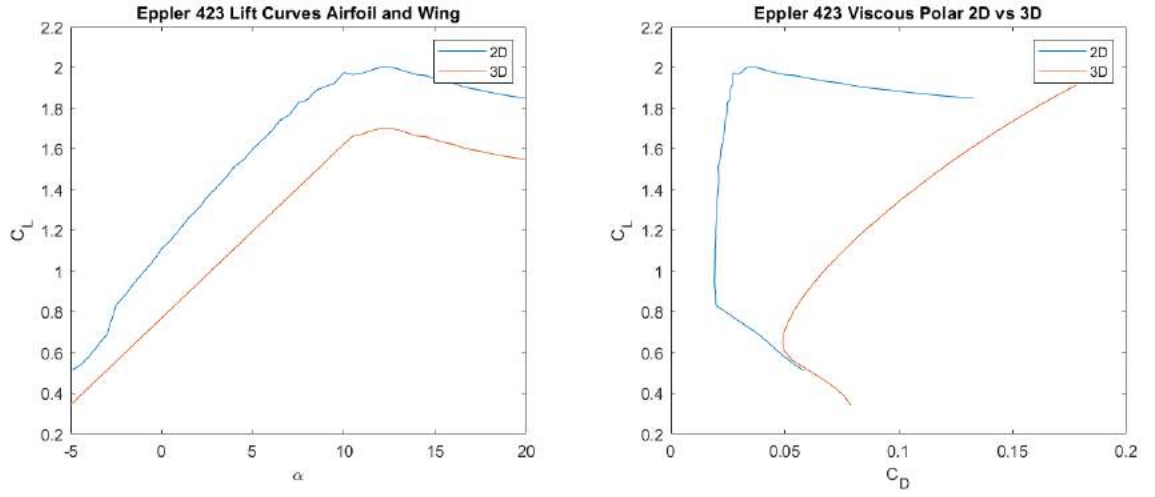


Figure 5: Lift and Drag Polars for Eppler 423

Various designs were explored for the wing; the design matrix is shown in Table 2. The final design is a configuration with two composite sandwich spars and a small carbon fiber tube spar near the trailing edge of the wing. Light balsa ribs are spaced evenly along the length of the wing. Past testing has shown limited benefits in increasing the number of fabric layers beyond two per side. The sandwich composite consists of two layers of plain weave carbon fiber on either side of a 1/8" balsa core (see Figure 6). The orientation of the layers strengthens the spar against both bending and torsional stress. The spars are constructed with two half-spans for transportation and accessibility for wiring.

Table 2: Trade Study for Wing Composition

Wing Configuration	Weight	Manufacturability	Cost	Strength/Durability	Drop Mech Compatibility	Total
Ribs with Basswood Spars	3	4	4	2	4	3.25
Ribs with Carbon Fiber Rods	3	4.5	2	4	2	3.125
Ribs with Composite Sandwich Spars	4	3	3	4	4	3.65
Foam Core with Carbon Fiber Layup	4	2	2	3	1	2.6
Importance	0.25	0.15	0.2	0.25	0.15	1

0°/90°
+45°/-45°
1/8" balsa
+45°/-45°
0°/90°

Figure 6: Composite Laminate



Figure 7: Wing Assembly

To verify the structure of the wing, calculations were done to check the bending stiffness of the spars. The spar located closer to the leading edge carries most of the bending load. Below is a plot that shows lowest safety factor of the layers in the laminate. Bending stiffness was calculated using the following equation:

$$H = \frac{b}{3} \sum_{i=1}^n (E_{x_1 x_1})_i [(x_2)_{i+1}^3 - (x_2)_i^3] \quad [1]$$

$(x_2)_i$ takes into account the thickness of the layers. This provides a weighted average of Young's modulus of the various layers.

Figure 8 shows how safety factor varies with load factor. The expected loading conditions in flight leave room for a significant safety factor.

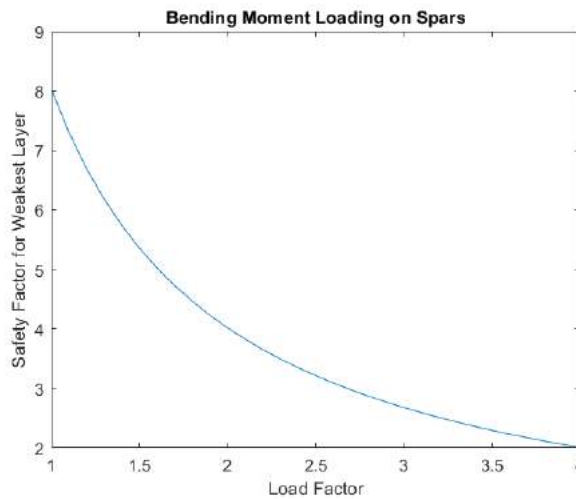


Figure 8: Spar Bending Safety Factor

4.3 Colonist Delivery Aircraft

4.3.1 Design Process

AMAT considered three major components in the design of the CDA (Icarus): total weight of aircraft, number of colonists delivered, and costs in its manufacturing. AMAT utilized decision matrices to organize various design options and evaluate their advantages and disadvantages to decide CDA configurations. Icarus' design is broken down into three main sections: the wings, fuselage, and empennage. AMAT determined the importance of each category by evaluating available resources and team expertise. Tables 3 and 4 showcase two of the design matrices that AMAT utilized during Icarus' design process.

Table 3: Design Matrix for Wing Configuration

Wing Configuration	Manufacturability	Previous Experience	Stability	Survivability	Weighted Totals
Delta Wing	1.5	1	3.5	3	1.9
Rectangular	4	4	3	2	3.6
Dihedral Rectangular	3	3.5	4	2.5	3.3
Bi-Wing	3.5	2	3	2	2.8
Importance	.40	.30	.20	.10	1.00

Table 4: Design Matrix for Empennage Configuration

Empennage Configuration	Weight	Previous Experience	Manufacturability	Survivability	Weighted Totals
Conventional	3.5	4	4	2.5	3.6
T-Tail	3	2.5	2.5	2	2.7
V-Tail	4	2.5	3	3	3.4
Importance	.50	.20	.20	.10	1.00

4.3.2 Wings

AMAT opted for a straight rectangular wing for its simple manufacturability. Though this configuration does not grant the lateral stability of a dihedral wing, the straight wing was much simpler for manufacturing multiple instances. The high-wing configuration grants lateral stability to the CDA and adds a ground clearance height for the wings avoiding their destruction at landing.

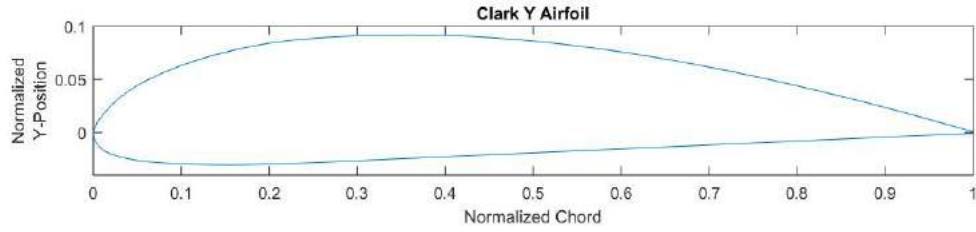


Figure 9: Clark Y Airfoil

AMAT selected the Clark Y airfoil for Icarus' wings, because of its reasonable manufacturability at the CDA scale; Clark Y airfoil is shown above in Figure 9. Airfoil and wing characteristics were analyzed using XFLR5. AMAT conducted aerodynamic analysis with Reynolds number range of $1 - 3E5$ based on previous given preliminary chord values, and historical atmospheric data of Van Nuys, California. A $C_{L,max}$ of 1.40 was tabulated for the Clark Y. Through preliminary predictions of Icarus' release airspeed, between 30-50 ft/s, and its maximum weight of 9 ounces, an aspect ratio of 10 was selected to minimize induced drag while limiting the wings' volume. A final high wing configuration of chord length of 2.5 inches, and half span of 12.5 inches is used.

4.3.3 Empennage

AMAT selected a conventional tail for its simplicity in design and manufacturing. AMAT opted to only include elevators as the control surfaces on the CDA's empennage. Only one servo motor was incorporated for the elevators, taking advantage of their rotation about the same axis in the same direction. While the vertical stabilizer was considered to have a rudder control surface, adding an additional motor in the empennage decreased the CDA's static margin, and increased its weight. AMAT prioritized the roll and pitch motion of the CDA over its yaw motion to keep its weight at a minimum.

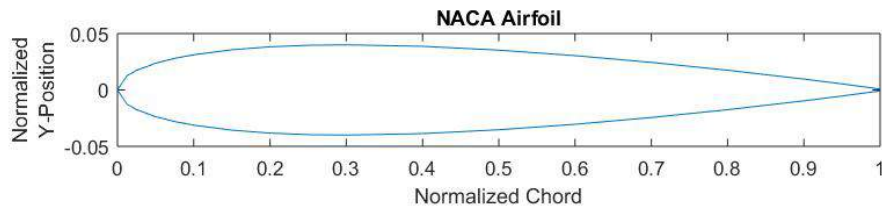


Figure 10: NACA 0008 Airfoil

The NACA 0008 airfoil (see Figure 10) was selected for the horizontal and vertical stabilizers' designs. The elevators and rudder were finalized to have a chord length of 1.6 inches and span of 4 inches. The horizontal stabilizers are equipped with elevators which allow the CDA to change its angle of attack and control its sink rate. Both stabilizers are both made from polyurethane

foam, reducing the tail's weight; and its rigidity was not prioritized since they will not bear significant aerodynamic loads.

4.3.4 Fuselage

Icarus' fuselage consists of a rectangular box large enough to carry its electronic components and sensors, with a colonist cabin positioned just below the electronics compartment, as shown in Figure 11. The driving factor around Icarus' fuselage design was to be able to fit all that is necessary for the glider to fly with the least volume and weight possible. These include the battery, control board, airspeed sensor with pitot tube, and the RC receiver in case a manual override is necessary during the mission. The number of colonists depends on the remaining weight allowed without surpassing the 9-ounce maximum. Similar to the wings and empennage, simplicity in the fuselage design was crucial for its repeatability in manufacturing.

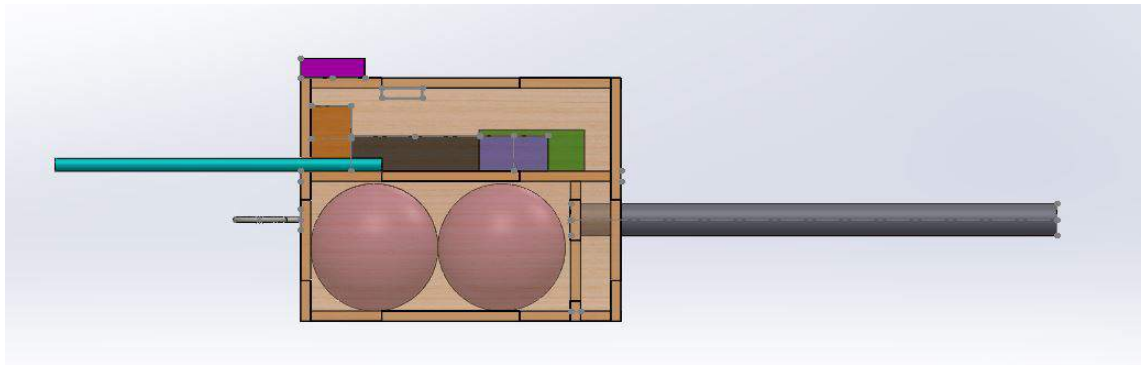


Figure 11: CDA Fuselage

The fuselage box consists of 1/8 inch thick basswood panels assembled together to fit the electronics compartment, a two-colonist cabin, as well as the carbon fiber tail boom to attach the empennage. The bottom panel of the CDA fuselage is removable so the colonists can be seen and finger-counted at competition. Icarus' fuselage top panel is also removable for easy replacement of electronic components. AMAT chose basswood for the box panels due to its ease of manufacturability and high rigidity. A carbon fiber tube was selected for the boom to minimize weight, to maintain the aerodynamic center aft of the center of gravity in front of the aerodynamic center, to maintain a positive static margin, and to be survivable. Through stability tests on XFLR5 iterated models and SolidWorks CAD models, Icarus' fuselage was finalized to have a colonist cabin capable of fitting two colonists.

4.4 Electronics

4.4.1 Power Circuit

The power circuit is connected to a motor which provides the mechanical power to operate and maneuver the main plane. The chosen flight battery specifications include a 6-cell configuration and features a 5000 mAh capacity, which allows a 8.88 minute flight.

$$\frac{Battery\ Capacity(Ah)}{Current\ Draw(Amps)} \cdot 60 = Flight\ Time(minutes)$$

In addition, the power circuit contains a power limiter. The electronic speed controller (ESC) is rated at 70 amp as the motor chosen is rated at 65 amp. This allows a safety margin to prevent the ESC from failing. An arming plug passes power to the ESC, which also has a battery elimination circuit (BEC), to provide 5.5 V to the flight controls. The power circuit schematic is shown below in Figure 12.

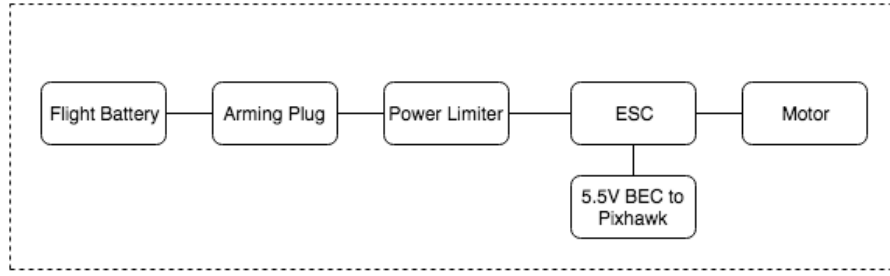


Figure 12: Power Circuit

4.4.2 Data Acquisition System

A PixHawk v1 board running ArduPilot operates the main plane's data acquisition and flight stabilization systems. AMAT selected this system as it offers support with a variety of sensors, telemetry, and flight stabilization. A laptop running Mission Planner is used as the ground station. Mission Planner was modified to display telemetry data per competition rules. The PixHawk contains an on-board gyroscope, barometer (resolution of .32ft), and compass. Airspeed data is provided by an analog airspeed sensor connected to a pitot tube. The system also features a GPS and redundant compass to assist with targeting. The PixHawk is powered by a 4-cell LiPo battery that provides a constant 5 V to the board and all sensors via a power module.

The FPV system allows the ground station to acquire real-time flight video from the plane. A 5.8 GHz AKK TS832 transmitter module located on the aircraft communicates video data

with a RC832 receiver on the ground. The capture card on the ground station converts the analog signals received by the FPV ground station receiver to digital video. The DAQ circuit schematic is shown below in Figure 13.

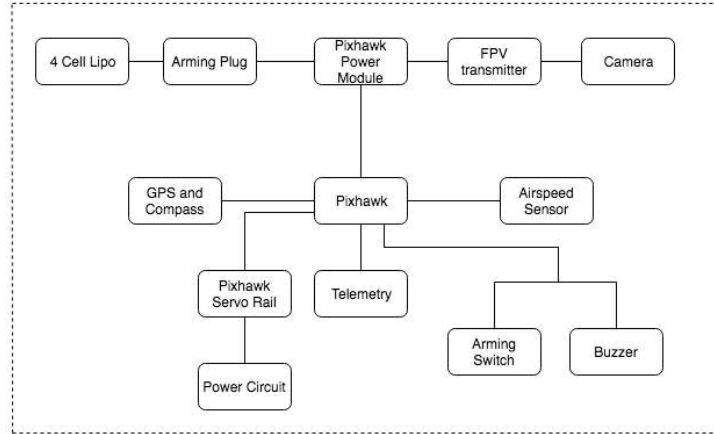


Figure 13: Data Acquisition System

4.4.3 CDA Circuit

The advanced class explicitly requires that the CDA be autonomously guided and un-powered with a manual override option in case of an emergency. Thus, AMAT selected the OpenPilot CC3D Revo board integrated with an on-board gyroscope and compass. The OpenPilot board is loaded with the ArduPilot software configured for gliding.

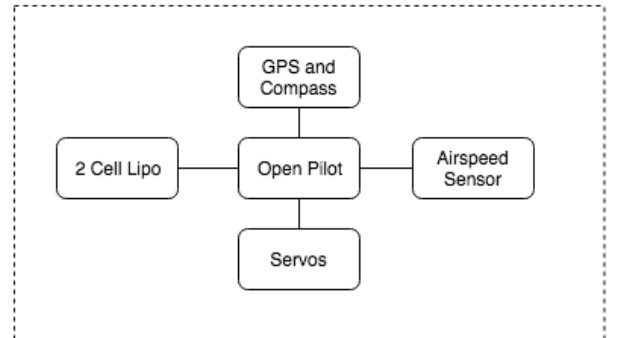


Figure 14: CDA Circuit

AMAT utilized ArduPilot software to determine airspeed, location, and commands on the control surfaces to modify the state of the CDA. The CDA is equipped with a pitot tube, analog airspeed sensor, and GPS module connected to the board; an RC receiver is also included for manual override. The OpenPilot is powered by a 2-cell 300mAh LiPo battery. The CDA circuit schematic is shown below in Figure 14.

4.5 Drop Mechanism

4.5.1 Dynamic Payloads

The drop mechanism is broken into three independent mechanisms, each corresponding to one of the payloads carried by the main craft.

Initially, AMAT considered a sling-type retention mechanism for the habitat. Although similar to previous drop mechanisms, it was deemed undesirable because the loose fabric was liable to flutter and the habitat could possibly strike the landing gear as it fell from the wing root. The sling was replaced with a solid acrylic claw-type mechanism. This allowed the habitat drop mechanism to be mounted further out on the wing, and removed the chance self collision.

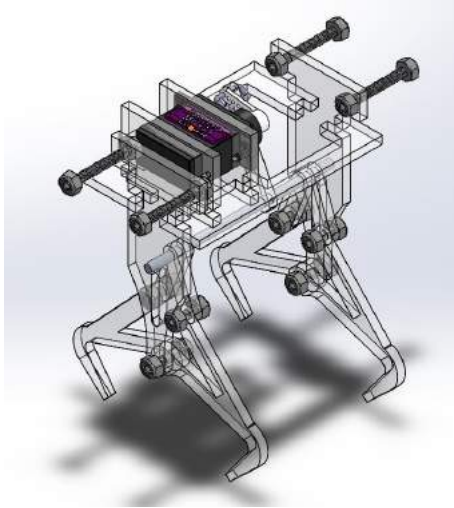


Figure 15: Habitat Drop Mechanism Open

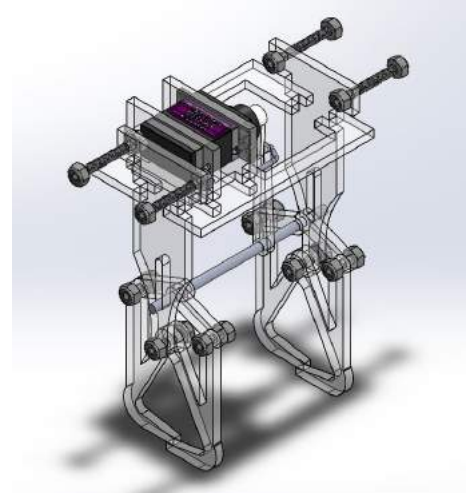


Figure 16: Habitat Drop Mechanism Closed

The claw apparatus under the wing encircles the tail of the habitat. The triangular opening is split down the middle into two hooks, joined at the top by an axis of rotation. A servo motor connects to the hooks via a link on the outside of the hook. The links are drawn upward by the servo, lifting the outside of the hooks upward along with them. The hooks rotate until they no longer contain the tail. This releases the football.

Similar to previous designs, the water bottle drop mechanism is a moving pin holding up a flexible cloth retaining sling. While the size and rigidity of the bottle are different than the previous competitions' payloads, the operating principle is similar, and thus a familiar design was chosen. The payload is retained in the lower center of fuselage by the sling. This sling is held up on one side of the fuselage by two static mounting points and on the other side by a single removable pin. When the pin is pulled out by a servo, the sling is released on one side and the water bottle is released from the fuselage.

The CDA is placed in a slot near the underside of the parent crafts fuselage. The CDA's wings rest on a lower ledge in the slot. To retain the CDA before release, a member runs from above the CDA through a loop on the front of the it. This prevents rearward movement. The member is L shaped, affixed by pins into a long guide slot running fore and aft. A rotating servo using a linking arm pushes the pins and vertical member along the slot until the CDA has

cleared the ledge. The CDA is then able to drop off of the member. The last portion of the slot angles up which forces the vertical member to tilt slightly back at the end of travel. The CDA then slides down it.

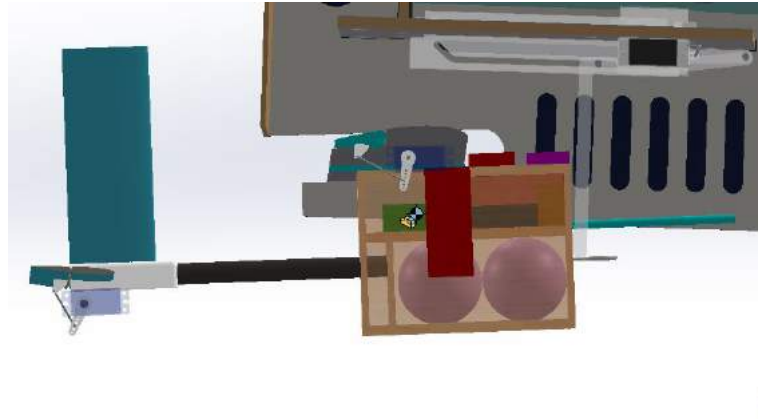


Figure 17: CDA Drop Mechanism

All components of the drop mechanisms, besides axles, are made of acrylic. Acrylic is both lightweight and rigid at small component size. Additionally it may be laser cut. Axles with loosely rotating components on them use standard all thread and lock nuts. For sliding components with higher friction, smooth aluminum rods are used.

4.6 Empennage

The U-tail empennage was designed to maximize streamline profiles and ensure structural stability while maintaining the required aerodynamic stability of the aircraft. In the past, AMAT had selected a conventional tail, but had struggled with finding an effective solution for joining the empennage to the boom. The U-tail allows for a smooth and streamline transition between the boom and horizontal tail as well as maintaining structural support. The boom attaches to the empennage by inserting into the slot cut out of the 3-D printed empennage mount and two spars insert through the mount and boom. The location of the boom and empennage keeps the horizontal tail below the wake of the wings.

Table 5: Trade Study for Empennage Configuration

Empennage Configuration	U-Tail	Conventional	T-Tail	V-Tail	Importance
Manufacturability	5	4	3	2	.35
Weight	3	3	4	5	.25
Complexity	4	5	3	1	.25
Previous Experience	4	4	2	1	.10
Survivability	3	3	2	4	.05
Weighted Totals	4.05	3.95	3.1	2.5	1

Shown in Figure 18, the U-tail design features a NACA 0012 airfoil made from panels of hollowed out foam supported by 2 carbon fiber spars connected together by 3-D printed joints. The symmetric NACA 0012 airfoil allows for both upwards and downward lift to be created due to the induced angle from the control surfaces. The elevators and rudders consist of a built up rib design using laser cut balsa wood coated in UltraCote to reduce the weight. The chord of the empennage is 8 inches with a 10.5 inch center joint to properly fit around the boom diameter. The elevators and rudders take up 43.75% of the chord to allow for optimum control during extreme flight conditions.

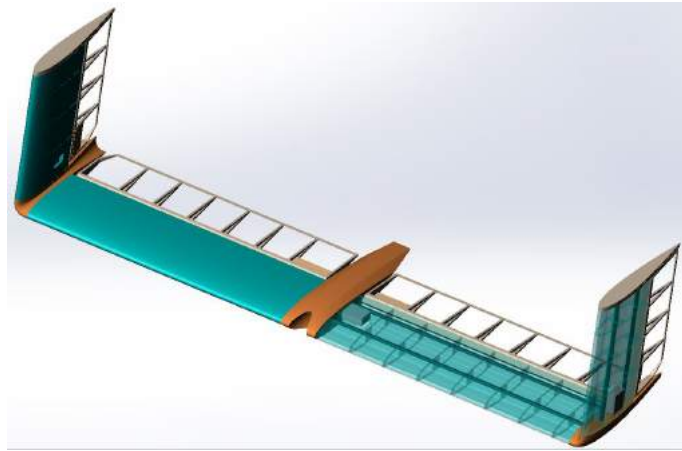


Figure 18: SolidWorks CAD Render of Exposed U-tail Empennage

The foam core was chosen for its low cost, strength, and simplicity in assembly. The only downside to the composition is the small increase in weight to the empennage. The spars will be the main structural strength of the empennage, but the foam will assist with adhering the UltraCote as well as resistance against torsional bending.

Table 6: Trade Study for Empennage Composition

Empennage Composition	Foam Core	Ribs with Foam Leading Edge	Ribs with 3-D Printed Leading Edge	Importance
Manufacturability	4	3	2	.25
Weight	3	5	3	.25
Strength	4	3	2	.25
Complexity	5	3	1	.20
Cost	5	4	3	.05
Weighted Totals	4.00	3.55	2.1	1

AMAT decided to 3-D print the connector joints out of PLA. PLA offered a strong and inexpensive option that would be easily manufactured 3-D printing also allows for components to be created with non-uniform density, which means non-structural portions of the components can be hollowed out to reduce the mass of the empennage.

4.7 Fuselage

AMAT's primary consideration in fuselage configuration selection was the accommodation of large volume payloads like the CDA and water bottle. As a result, the CDA's configuration and its drop mechanism design played a key role in selecting a fuselage configuration. The decision to use a rectangular wing and conventional tail in the CDA made a box design ideal. This configuration allows for a large drop bay for the water bottle and a slotted bay for the CDA, while being easy to manufacture. This configuration, however, is heavy and high-drag. The high weight is acceptable as weight can be reduced with carbon fiber construction and use of lightening holes. High drag is a desirable quality for AMAT's planned slow speed mission.

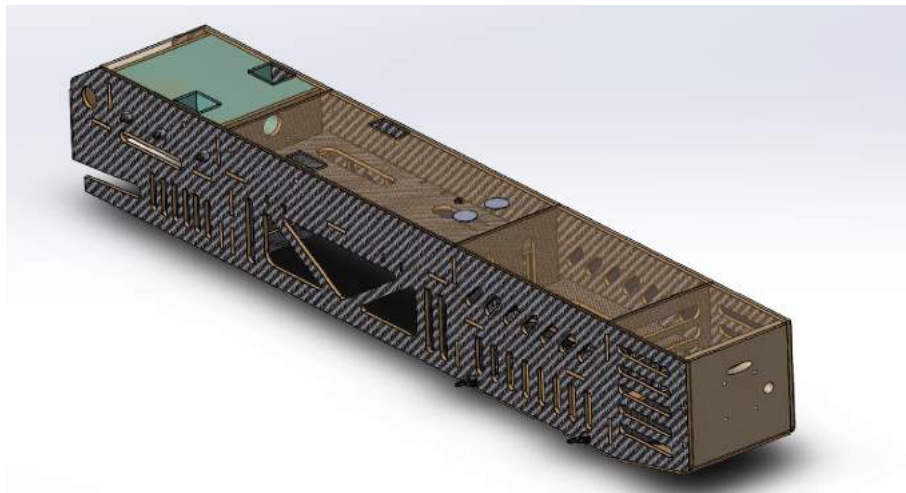


Figure 19: SolidWorks CAD render of the fuselage with bulkheads and side panels showing

Table 7: Trade Study for Fuselage Configuration

Fuselage Configuration	Box	Flat Plate	Circular	Importance
Available Space	4	3	1	50
Manufacturability	4	3	2	.30
Weight	2	3	3.5	.5
Survivability	3.5	4	3	.15
Weighted Totals	3.825	3.15	1.725	1

In order to help minimize the high weight of a box configuration, AMAT constructed the aircraft's fuselage using single ply carbon fiber layed up on balsa wood. This construction is ideal for its high strength-to-weight ratio. The fuselage core structure consists of two large side panels coupled together with four bulkheads. The bulkhead's primary purposes are to provide structural strength and to separate the different compartments of the fuselage. In addition, horizontal bulkheads divide some of the compartment into two horizontally while providing additional strength.

The compartments need to be large to accommodate the payloads. Larger compartments and fewer bulkheads necessitated greater rigidity in the carbon fiber balsa layup. AMAT accomplished this by using 3/16" balsa. The firewall is constructed from plywood. The lower aft and lower center compartments contain large amounts of space for the CDA and water bottle respectively; the bottom of the fuselage is excluded for those sections to simplify the dropping process. The upper and forward compartments carry electronics, avionics, and static payload.

4.7.1 Static Payload

The aircraft carries 2 lbs of static payload which are constructed of latex gloves filled with ball bearings, located in the top of the fuselage under the wing. AMAT traditionally uses this as static payload as it's easy to create large quantities of weight.

4.8 Landing Gear

The main problem with the landing gear is the size requirement. The overall size of the plane required relatively high landing gears to be designed to allow for the expected angle of attack at take off. Due to the required height, tricycle landing gears were chosen for the base design. The front gear was designed to be steerable per competition requirements.

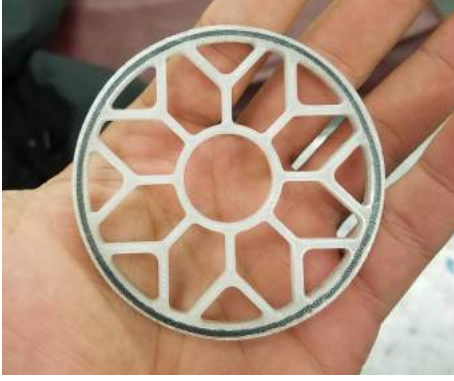


Figure 20: Nylon/Carbon Fiber Composite Landing Gear Wheel

The wheel design was based off of proven previous year designs that maximize the strength to weight ratio. The wheels are 3D printed, which allows for the complex shape to be easily manufactured. A rubber o-ring is used on the outside to dampen the landing loads and to make the taxing smoother.

For the rear landing gear, a trade study was conducted to select the ideal support material. The factors of consideration were strength, density, elasticity, cost and manufacturability; all had the same weighting factor.

Table 8: Trade Study for Landing Gear Material

	Strength	Density	Elasticity	Cost	Manufacturability	Total
Wood	0	0.8	0	1	0.7	2.5
Aluminum	0.7	0.5	0.2	0.8	0.9	3.1
Steel	0.7	0	0.9	0.7	0.6	2.9
ABS Plastic	0	1	0	0.8	1	2.8
Carbon Fiber	1	0.6	1	0	0	2.6

Aluminum was the best material, so it was selected to be the main material for the rear landing gear. The front gear needs to take a lot more compressive loads during landing. Steel was chosen to be the material for it since it has a higher elasticity value. Carbon fiber would be a better material from the strength and elasticity perspective, but it comes with high costs and manufacturability concerns.

5 Analysis

5.1 Analytical Tools Used

AMAT primary used XFLR and XFOIL to analyze the performance of various potential wing configurations. XFLR was also used to perform static and dynamic stability analysis for both aircraft. MATLAB programs were written to perform payload and performance analysis.

5.2 Dynamic and Static Stability

5.2.1 Longitudinal Stability

Longitudinal stability is important for the main plane as aircraft at this scale have low moments of inertia relative to full scale aircraft. The plane must be steady to perform accurate drops, so the team prioritized stability over maneuverability. The complex mission results in five different loading conditions over the course of the competition. Using XFLR and MATLAB, the team determined static margin in each of the loading conditions to ensure stability throughout the course of the mission. Payload placement was done with stability in mind: center of gravity varies by less than inch over the course of a flight. The static margins for the different configurations are detailed in Table 9.

To satisfy static longitudinal stability requirements, the following must hold true:

$$SM = -\frac{C_{M\alpha}}{C_{L\alpha}} = \bar{x}_{ac} - \bar{x}_{cg} > 0$$

Table 9: Static Margin for Various Configurations

Loading Condition	$x_{CG}(ft)$	$x_{NP}(ft)$	$SM(\%)$
Empty	2.263	2.608	10.5
Static	2.255	2.608	10.7
CDA, Nerf, Water, Static	2.293	2.636	10.4
Nerf, Water, Static	2.199	2.608	12.4
Nerf, Static	2.25	2.608	10.8

For the purposes of this report, dynamic stability analysis results for the critical fully loaded configuration is shown below. Results from the longitudinal stability analysis give a damping ratio of 0.714 for the short period, which falls between 0 and 1, indicating positive dynamic stability. The phugoid mode is slightly unstable, but the long period of the response ensures that the pilot has sufficient time to respond.

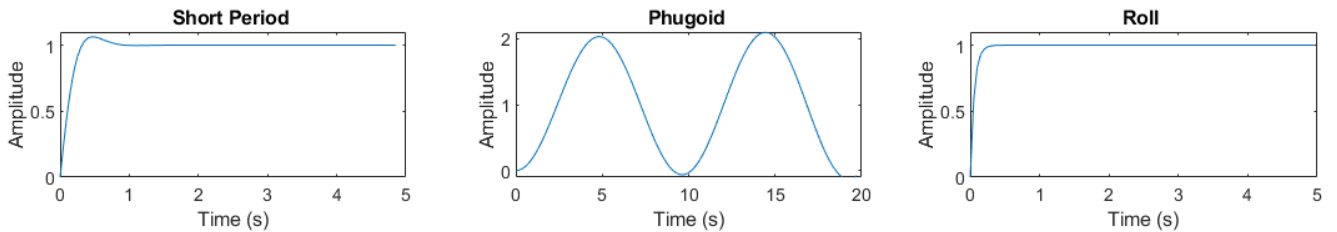


Figure 21: Short Period, Phugoid, and Roll Stability Plots

5.2.2 Lateral Stability and Directional Stability

AMAT ensured the lateral stability of the aircraft by selecting a high wing configuration and keeping the aerodynamic center above the center of gravity. Other methods of keeping lateral stability such as wing dihedral and wing sweep back were avoided to simplify manufacturing. In addition, a PixHawk flight controller assists the pilot with lateral stabilization. AMAT used twin vertical stabilizers to ensure a high vertical tail area and maintain directional stability.

5.3 Control Surface Sizing

Ailerons were sized to gust loading: historical maximum wind speeds data from Van Nuys, CA in April revealed a max wind speed of 33 ft/s in the past 5 years. Ailerons were sized to a safety factor of 1.48 (48.8 ft/s) giving a $C_{L_{\delta\alpha}}$ of 0.314. The aspect ratio of the ailerons was increased from prior years to reduce potential slop and reduce load on servo motors. Aileron sizing was iterated using XFLR and MATLAB until the ailerons were determined to have sufficient control authority in each of the loading conditions. The ailerons measure 4.5" in chord and 18" in span on the outboard of the wing.

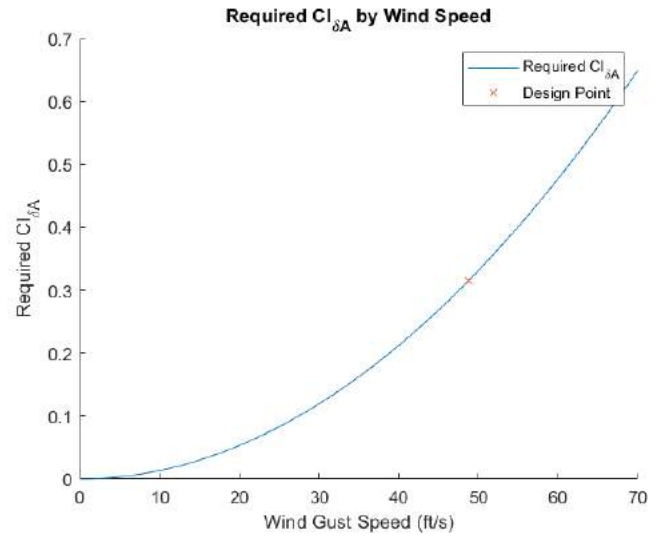


Figure 22: Aileron Sizing for Gust Loading Conditions

5.4 Servo Sizing

Servos must be sized appropriately to generate torque to actuate control surfaces of the aircraft. The below equation was used to calculate maximum torque load required:

$$\tau = \frac{MW \cdot P}{4RT} \frac{\sin(S_{max}) \tan(s_{max})}{\tan(s_{max})} 2C^2 V_{max}^2 \dot{S} F$$

MW is molecular weight, P is air pressure, T is the temperature, R is the ideal gas constant, S is the max control surface deflection from neutral, s is the maximum servo deflection from neutral, C is the control surface chord, V is the max speed, and SF is the chosen safety factor.

The servos were sized for the various components and an appropriate servo was selected

to provide a safety factor. This is summarized in Table 10.

Table 10: Servo Sizing

Component	Required Torque (<i>lbfin</i>)	Provided Torque (<i>lbfin</i>)
Ailerons	1.18	2.58
Rudder & Elevator	0.5948	1.09
CDA aileron	0.0011	0.1157
CDA elevator	0.0024	0.1157

5.5 Drag, Thrust, Takeoff, and Lifting Performance

AMAT determined aircraft performance at the most critical phases of the mission through analysis and testing. A zero lift drag coefficient breakdown of the entire main aircraft based on Reference 2 can be seen in Figure 11.

Table 11: Zero Lift Drag Breakdown

Component	C_{D_0}	Component	C_{D_0}
Fuselage	0.0055	Wing	0.0136
Horizontal Stabilizer	0.0031	Vertical Stabilizer	0.0014
Tail Boom	0.0008	Landing Gear	0.0042
Motor	0.002	CDA(stowed)	0.004
Total	0.0346		

One major consideration for thrust calculations was the SAE required power limiter. Due to the limiter's unknown effect on torque and engine speed, static thrust tests had to be performed with various propellers. AMAT verified that data from the propeller manufacturer aligned with the results of the thrust test, and used the data to create a dynamic thrust curve. The curve with the selected APC 13x6.5E propeller is seen in Figure 23 .

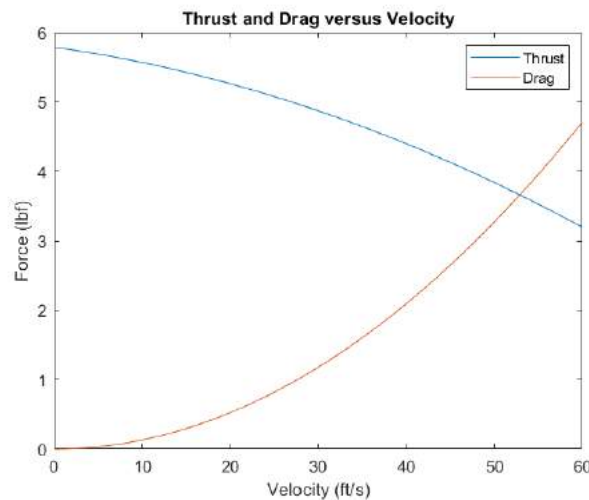


Figure 23: Dyanamic Thrust Curve

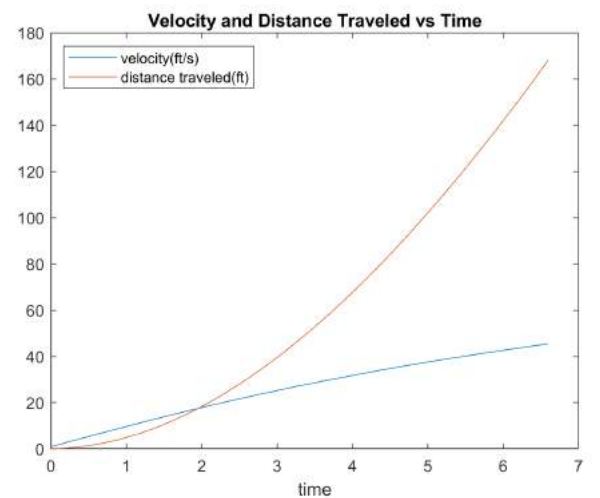


Figure 24: Take off distance and velocity

The lift, drag, and thrust results at takeoff and cruise are summarized in Table 12.

Table 12: Lift, Drag, and Thrust during Cruise and Takeoff

	Lift(lbf)	Drag(lbf)	Thrust(lbf)
Takeoff	22	2.25	6.1
Cruise	18	3.27	3.84

This data allows AMAT to determine takeoff performance at full payload. Assuming a takeoff speed just above stall at 45 ft/s and conditions at the competition site, AMAT calculated estimated runway takeoff length to be 172 feet according to analysis performed in MATLAB. Figure 24 shows aircraft velocity and runway distance traveled.

5.6 Mass Breakdown

Table 13: Mass Breakdown

Component	Mass (lb)	Component	Mass (lb)
Fuselage	2.58	Empennage	1.30
Boom Spar	0.70	Gear	1.46
Wings	2.86	Motor	0.80
Drop Mech	0.18	Electronics	2.24
Static	2.00	Dynamic	3.87
Total	17.99		

The total predicted weight of around 18lbs under the maximum of 25lb. This allows for some variance in manufacturing, such as increased epoxy, wiring, and other miscellaneous component weight. It also leaves margin for thrust performance at competition.

5.7 CDA Analysis

5.7.1 Lift Performance

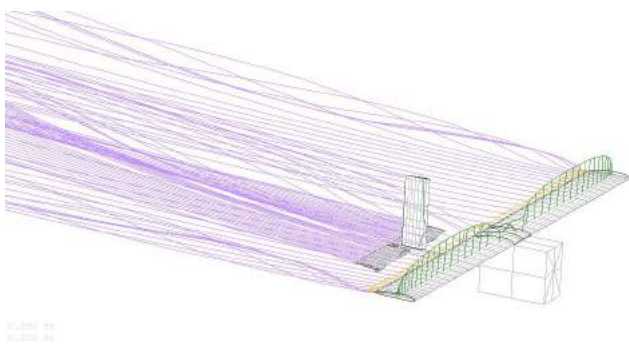


Figure 25: Aerodynamic Visual of CDA

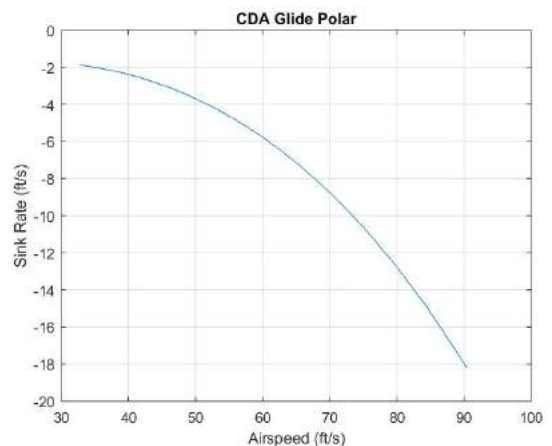


Figure 26: CDA Glide Polar

Because of the mission requirements for the CDA release and landing, AMAT aimed for a relatively low glide ratio and efficiency. This required the CDA to have low lift to drag ratio, which justified the rectangular shape of the fuselage. Utilizing XFLR5 the lift and drag coefficients were obtained with relation to angle of attack at the desired Reynold's numbers. Utilizing MATLAB software, these lift and drag polars were transformed into a glide polar under no gust loading and fully-loaded with colonists, using the historical atmospheric conditions of Van Nuys, CA in April. Figure 26 shows the glide polar for the 3D CDA model.

5.7.2 Stability

Icarus' center of gravity (CG) position in relation to the aerodynamic center of its wings and elevators greatly affect its longitudinal stability during its flight; the aircraft's longitudinal stability is what allows it to return to its equilibrium orientation after being affected by any perturbations during flight. A careful arrangement of Icarus'

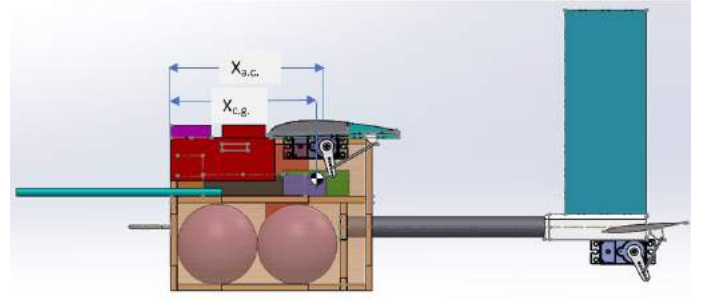


Figure 27: Side View of CDA

electrical components and sensors, as well as the boom's length significantly influenced the CDA's CG along its forward axis. Additionally, Icarus' elevators are angled down 5 degrees from the longitudinal axis, to provide a downward force to counter the moment created by Icarus' weight about its wings' aerodynamic center. Stability analysis was conducted through XFLR5 for Icarus' design to justify its aerodynamic and inertial design and virtually confirm its longitudinal stability. Similarly, Icarus' high wing was designed to maintain its lateral stability so it can be autonomously guided to its landing zone with few control surface corrections. Dynamic stability tests revealed that Icarus, though stable, is underdamped which requires it to input control surface commands to return to equilibrium. Table 14 displays Icarus' dynamic longitudinal stability frequencies in the short period mode and phugoid mode.

Table 14: Icarus' Dynamic Stability

Mode	Natural Frequency (rad/sec)	Damped Frequency	Damping Ratio
Phugoid	.157	.157	.007
Short-Period	2.442	2.259	.380

6 Manufacturing

6.1 Composite Manufacturing



Figure 28: Carbon Fiber Layup on the Spars

The manufacturing of the composites is done through vacuum assisted hand layup. Carbon fiber mats are saturated with epoxy before adding the next layer of the sandwich. Different parts utilize varying laminates. A vacuum was applied to the layup, with a pressure of around 20 mmHg. This allows for uniform pressure to assist in cure and help remove excess epoxy. A low viscosity, thermoset epoxy resin system of 600 cps was selected for ease of application and saturation of large composite pieces.

G code was generated using Autodesk Fusion 360 to cut the parts to the correct dimensions. The wing spars and fuselage composites were machined down to size using by a CNC Shopbot.

The CDA's foam core wings are also reinforced by a vacuum assisted carbon fiber-epoxy layup to minimize the wing's deflection from the wind loading. The inner carbon fiber layer is $\pm 45^\circ$ to reduce torsion deflections. The outer carbon fiber layer is 0/90 degrees to take the axial stress from the wing bending due to lift and drag loading.

6.2 Additive Manufacturing

Additive manufacturing allows for the creation of complex geometries that traditional machining could not replicate. Additive manufacturing will be utilized in both the empennage and the landing gears.

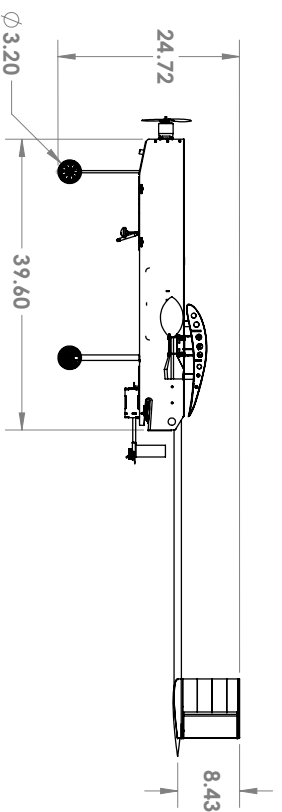
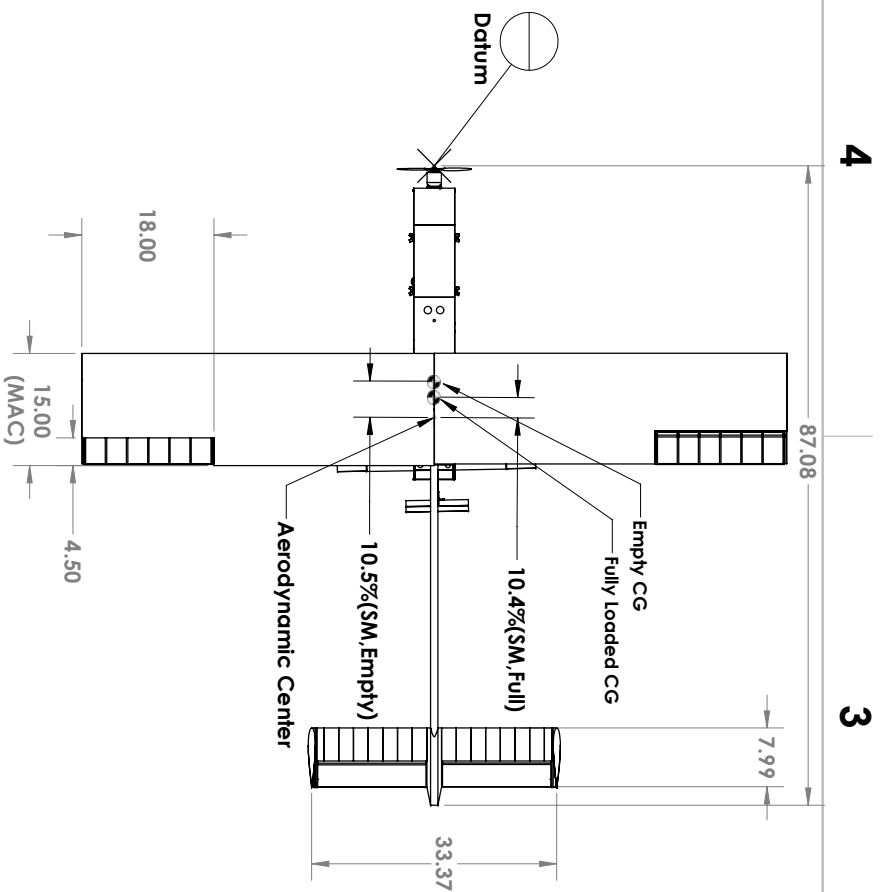
The empennage joints will be printed out of PLA. The landing gear benefited from the use of nylon composite with carbon fiber reinforcement. As seen in Figure 20, the carbon fiber inlay strengthens the landing gear so that less material is needed to maintain structural stability and ultimately reduces weight on the aircraft. The technologically advanced composite additive manufacturing was used selectively for the landing gear wheels due to the price per print: nylon/carbon fiber composite prints cost over 40 times prints done with PLA.

7 Conclusion

The 2019 Advanced Modeling Aeronautics Team presents Daedalus and Icarus for submission to the 2019 SAE Aero Design West Advanced Class. With the support of the UC Davis Mechanical and Aerospace Engineering Department as well as several sponsors, AMAT worked hard to design, manufacture, and deliver a colonist and life support delivery system. AMAT utilized prior knowledge from coursework as well as external resources on aerodynamics and aircraft design in conjunction with custom code to guide plane development. By combining Icarus's autonomous flight capability with Daedalus's data acquisition system, the team will successfully complete the colonists delivery mission.

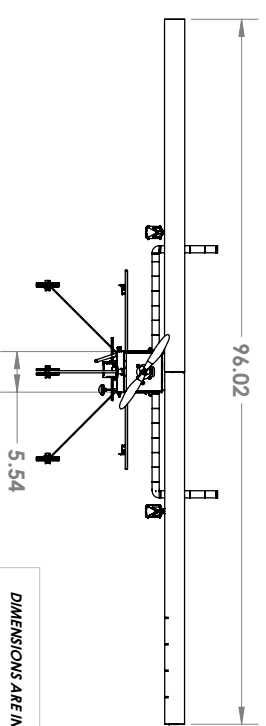
8 References

- [1] Bauchau, O. A. Craig, J. I. (2016). Structural Analysis: With applications to aerospace structures.
- [2] Nicolai, Leland, M (2009). Estimating R/C Model Aerodynamics and Performance

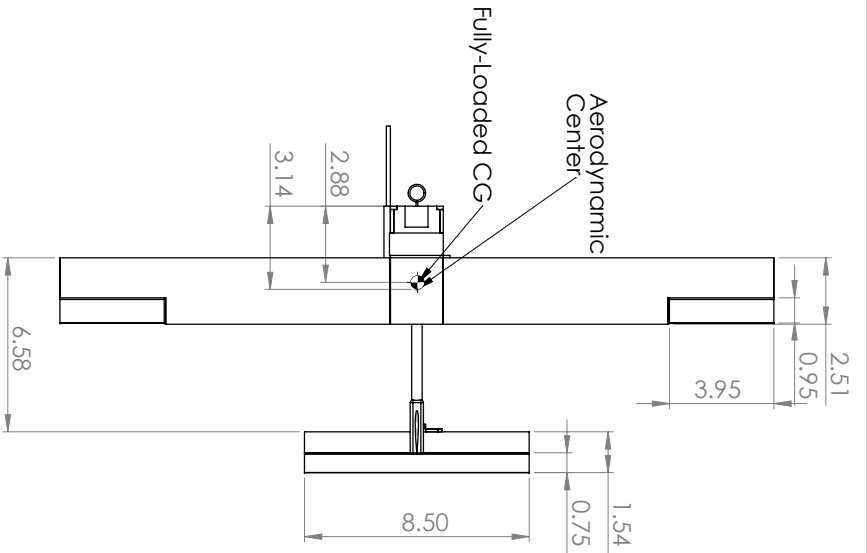


Component	Weight(lbs)	xCG(in)	Moment Arm (lb ² /in)
Motor	.80	1.43	1.14
Batteries (6s/4s)	(1.61/.26)	(14.04/19.83)	22.06/5.15
2x Nerf Football	.44	24.63	10.83
CDA	.50	38.49	19.25
Water Bottle	2.30	25.04	57.59
Flight Controller	.11	25.93	2.85

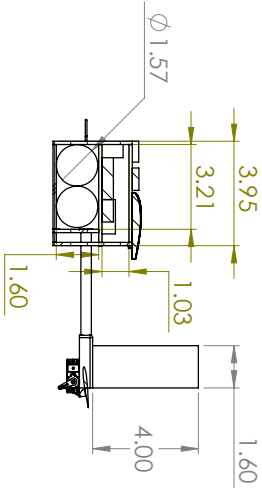
Wingspan	96.02 in
Empty Weight	12.8 lbs
Motor	Turnigy G40 500kv
Propeller	APC 13x6.5E prop
2x Wing Servo	Hitec 31311S, 42oz/in
4x Tail Servo	Smezza SG90, 17.5 oz/in
4x Drop Mech Servo	Scamming MG90S, 28oz/in
Nose Gear Steering	FullFunRC 9KG, 104.1oz/in
Flight Battery	6s lipo 5000 mah 30C
DAQ Battery	4s lipo 1200 mah



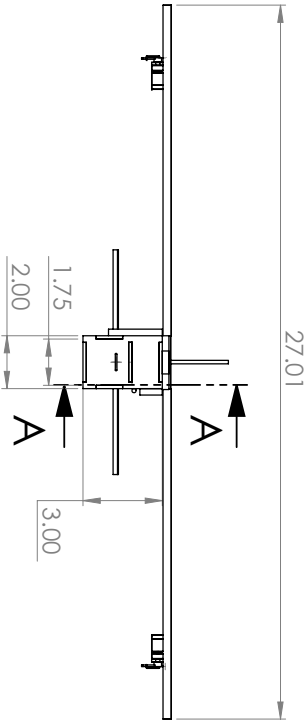
DIMENSIONS ARE IN INCHES. TOLERANCES: ± .01	
TITLE: UC Davis Team #218 Advanced Modelling Aeronautics Team	
SIZE Name:	REV
B Daedalus	2/24
SCALE: 1:18	SHEET 1 OF 1



Component	Mass (lb)	Moment Arm (ft) From Front Panel of Fuselage	Moment(ft-lb)
Fuselage Box and Boom	.1319	.2222	.0293
Wing	.1200	.2531	.0304
Empennage	.0186	.7196	.0134
Battery	.0438	.0311	.0014
Electronics (Board, Sensors, and Receiver	.0543	.1215	.0066
Servo Motors	.0775	.4074	.0037
2 Colonists (Maximum Capacity)	.0120	.1413	.0017
Unloaded CDA	.4926	.2423	.1194
Fully Loaded CDA	.5046	.2399	.1211
MAC	.2083 ft	Servo Type:	Hextronik HXT900
Unloaded CDA SM	.0946	Maximum Torque:	22.20 oz-in
Fully Loaded SM	.1061		Used ailerons and elevator



SECTION A-A



UNLESS OTHERWISE SPECIFIED:

TITLE:

UC Davis Team #218
Advanced Modeling
Aeronautics Team

UC Davis Team #218
Advanced Modeling
Aeronautics Team

DIMENSIONS ARE IN INCHES, FRACTIONS: TWO PLACES, DECIMAL: .02

SIZE: **B**

REV: **2/24**

SCALE: 1:5

WEIGHT: 0.506 lb

SHEET 1 OF 1